Research article

Development of a 3D Tissue Engineered Skeletal Muscle and Bone Co-culture System

Nicholas M. Wragg[1,2]

Diogo Mosqueira[1]

Lia Blokpeol-Ferreras[1]

Andrew Capel[1]

Darren J. Player[1,3]

Neil R. W. Martin[1]

Yang Liu[2]

Mark P. Lewis[1]

[1]School of Sport, Exercise and Health Sciences, Loughborough University, Loughborough, United Kingdom

[2]Wolfson School of Mechanical, Electrical and Manufacturing Engineering, Loughborough University

[3]Institute of Orthopaedics and Musculoskeletal Sciences, RNOH University College London Stanmore, United Kingdom

Corresponding Author: Dr. Nicholas M. Wragg, Centre for Biological Engineering, Wolfson School of Manufacturing and Mechanical Engineering, Holywell Park, Loughborough University, Loughborough, LE11 3TU, United Kingdom

E-Mail: n.m.wragg2@lboro.ac.uk

Keywords: Bone, co-culture, medium compatibility, skeletal muscle, tissue engineering.

Received: 25-03-2019; Revised: 05-07-2019; Accepted: 19-07-2019
This article has been accepted for publication and undergone full peer review but has not been through the copyediting, typesetting, pagination and proofreading process, which may lead to differences between this version and the Version of Record. Please cite this article as doi: 10.1002/biot.201900106.

List of bbreviations:
3D – Three dimensional
TE –Tissue engineered
HG-DMEM – High-glucose Dulbecco's Modified Eagle Medium
EMEM – Eagle's Minimum Essential Medium
FBS – Feotal bovine Serum
MPC – Muscle Precursor Cell
hOS – human osteosarcoma
GM – Growth medium
HA – hydroxyapatite
MEM - Minimal Essential Medium
OM – Osteogenic Medium
MM – Myogenic Medium
TBS – Tris Buffered Saline
PBS – Phosphate buffered saline
TRITC – tetramethylrhodamine
qRT-PCR – Quantitative Reverse Transcription Polymerised Chain Reaction
ALP – Alkaline Phosphate
4-MUP - 4-methylumbelliferyl phosphate
EDTA - ethylenediaminetetraacetic acid
MAC – metabolic activity per live cell

Abstract

In vitro three-dimensional (3D) tissue engineered (TE) structures have been shown to better represent *in vivo* tissue morphology and biochemical pathways than monolayer culture, and are less ethically questionable than animal models. However, to create systems with even greater relevance, multiple integrated tissue systems should be recreated *in vitro*. In the present study, the effects and conditions most suitable for the co-culture of TE skeletal muscle and bone were investigated. High-glucose Dulbecco's Modified Eagle Medium (HG-DMEM) supplemented with 20% foetal bovine serum (FBS) followed by HG-DMEM with 2% horse serum was found to enable proliferation of both C2C12 muscle precursor cells and TE85 human osteosarcoma cells, fusion of C2C12s into myotubes, as well as an up-regulation of RUNX2/CBFa1 in TE85s. Myotube formation was also evident within indirect contact monolayer cultures. Finally, in 3D co-cultures, TE85 collagen/hydroxyapatite constructs had significantly greater expression of RUNX2/CBFa1 and osteocalcin/BGLAP in the presence of collagen-based C2C12 skeletal muscle constructs; however, fusion within these constructs appeared reduced. This work demonstrates the first report of the simultaneous co-culture and differentiation of 3D TE skeletal muscle and bone, and represents a significant step towards a full *in vitro* 3D musculoskeletal junction model.

1 Introduction

Currently, *in vitro* bio-toxicity testing of developmental pharmaceuticals, biomaterials and medical devices is performed on *in vitro* monolayer cell culture models (ISO10993). Monolayer models are capable of identifying cytotoxic effects through morphological and biochemical assays, or by assessing changes in gene expression [1]. However, these results do not effectively translate across to *in vivo* tissue systems [1,2]. This is due to a general failure to accurately recapitulate the complex nature of native tissue structures and the biochemical pathways that accompany such architecture, therefore justifying the use of animal models [3–6]. Animal models clearly demonstrate complex tissue structures and pathways, although these models have accompanying high costs, contentious ethical considerations and results that do not always translate across species [7,8]. As such, there is a growing need for more complex *in vitro* models, which provide more representative structures and physiology than conventional cell cultures, without the complexities of animal research.

Development of increasingly relevant models has shown the potential of three-dimensional (3D) tissue engineering (TE) solutions for *in vitro* preclinical testing [2,9–12]. Engineered constructs require a cell source capable of forming the structures and processes associated with *in vivo* tissues. This is in addition to environmental conditions, such as a substrate/scaffold and specific nutrients, which enable the establishment of these characteristics. However, due to the very different physical structures of each of these tissues and hence, their culture conditions, *in vitro* 3D models of skeletal muscle and bone have yet to be cultured together.

Myogenic differentiation in both monolayer and 3D requires muscle progenitor cells, or myoblasts (MPCs), to exit the cell cycle. *In vitro*, this is generally met through a

reduction in serum content to induce cellular fusion [13–17]. Current 3D muscle models use this process in tandem with a scaffold to act as an extra-cellular matrix. This is typically a cell-seeded hydrogel, which is tethered during the setting of the hydrogel or during the culture, as MPCs delaminate and self-assemble between the anchor points [18–25]. MPCs align according to lines of isometric tension which are formed through cell mediated scaffold contraction over the culture period [26]. This helps to create highly aligned populations of myotubes which better represents *in vivo* structure than monolayer cultures [5].

TE bone models also utilise a scaffold and either an osteoblast-like cell line or a multipotent stem cell, for example a mesenchymal stem cell, to act as a source of matrix deposition and remodelling [27–29]. There are many different types of bone scaffold based on synthetic or naturally-derived materials [30–36]. Individually, each of these scaffold types have disadvantages, such as reduced cell affinity [28,37]. However, by combining materials to create a hybrid/composite scaffold, these disadvantages can be reduced or eradicated to assist in the formation of a more relevant bone-like model [38–41]. The addition of ascorbic acid, β-glycerophosphate and dexamethasone have been shown to increase RUNX2/CBFa1 expression and matrix production, as well as the formation of bone mineral in osteoblast/osteoblast-like cells [42].

By comparing the effects of reported skeletal muscle and bone medium compositions on both cell populations in monolayer and 3D, this work sought to establish conditions conducive to the co-culture of 3D tissue engineered skeletal muscle and bone towards the formation of an *in vitro* musculoskeletal junction (muscle-tendon-bone). This would greatly increase the physiological relevance of *in vitro* toxicology testing before *in vivo* studies and could aid in the understanding of musculoskeletal diseases.

2 Materials and Methods

2.1 Cell Culture

Cell populations were cultured under humidified atmospheric O_2 and 5% CO_2 conditions at 37°C (5% CO_2 in air). Medium compositions were based upon previous literature (Table 1) [16,43–46]. C2C12 murine MPCs (ECACC, UK) were expanded in M1. All experiments were conducted prior to passage 8. TE85 human osteosarcoma (hOS) cells (ATCC, UK), were expanded in M2; or growth medium (GM) as detailed for C2C12s (M1). All experiments were conducted prior to passage 60.

2.2 Media Composition Culture Comparisons

Proliferation Phase: Both cell lines were seeded at 4500 cells/cm² in 6 well plates and cultured for 4 days in M1, M2 or M3. Cells were lysed and processed for DNA and protein analysis at 24, 48 and 96 hours post seeding. Metabolic activity was measured at 96 hours and then samples passaged for live cell number and membrane integrity (viability). Brightfield micrographs were taken using a Leica DMIL LED light microscope prior to lysis for morphological analysis.

Differentiation Phase: Based on results of the proliferation phase cell culture, a single maintenance media (M1) was chosen to culture the cells prior to differentiating. Cells were cultured as detailed during the proliferation phase. Once confluent, cells were cultured in either osteogenic (OM) or myogenic (MM) differentiation media for 3 days. M2 was used as a control for the TE85s. Cells were lysed for analysis at 24, 48 and 72 hours post seeding.

2.3 Indirect Contact Co-culture of C2C12 MPCs and TE85 hOS

Polydimethylsiloxane (PDMS, Sylgard® 184 Elastomer) was pre-set in six well plates (Nunc) and cut to provide a central barrier approximately 0.5x3.5x0.5mm across the

wells (Figure 1). C2C12 MPCs and TE85 hOS cells were seeded separately at 4500 cells/cm^2 in 2.0mL of GM (M1) either side of the barrier and left to attach for 2 hours. GM (M1) was added to each well until the levels rose above the PDMS (*ca.* 6.0mL) and 2.0mL replenished daily. At confluency (*ca.* 72 hours post seeding), GM was removed and replaced with 1.0mL MM and 0.32mg/mL hydroxyapatite (HA) in MM to the C2C12s and TE85s respectively. Cultures were left for 2 hours at 37^{o}C/5% CO_2 in air to allow the HA to settle onto the TE85s. MM was then gently added to the well on top of the boundary to increase levels above the PDMS barrier (*ca.* 6.0mL). Cells were lysed for analysis after 3 days. Controls of MPC/hOS-HA, hOS-HA/hOS-HA, MPC/MPC, hOS+HA/hOS+HA and MPC/MPC with HA conditioned medium were set up simultaneously.

2.4 Tissue Engineered 3D Collagen Constructs

Skeletal Muscle Model: Skeletal muscle constructs were prepared according to an adjusted protocol [5,16]. Briefly, 10x Minimal Essential Medium (MEM) (Gibco) was added to 2.0mg/mL type-1 rat tail collagen (First Link, UK) and mixed thoroughly. This solution was then neutralised using 5M and 1M NaOH until a colour change from yellow to pink was observed. MPCs suspended in GM (M1) were then added to the collagen solution and pipetted into a defined setting area (15mm x 28mm) with bespoke anchor points, termed “A-frames” at either end (Figure 2). The final solution comprised 85% collagen, 10% 10x MEM and 5% cell suspension. Each A-frame consists of poly(ethelene-co-1-octene) plastic 10 count canvas mesh (Darice, US) bound together with 0.3mm stainless-steel wire (Scientific Wire Company, UK) to form a floatation bar. 0.3mm wire was used to create a hook which could be pushed into the floatation bar and hung over the side of the setting chamber to keep the construct stable.

Bone Model: HA solution and collagen/HA 3D constructs were prepared according to an adjusted protocol [47]. ***Hydroxyapatite Solution Preparation:*** 500mL of 130mM analytical grade ammonium phosphate tribasic trihydrate (NBS Biologicals Ltd) was added dropwise into 500mL of 210mM calcium acetate solution. The solution was continuously stirred and maintained at pH12 and 3°C by adding concentrated ammonium hydroxide and housing in a bath of iced water. The precipitate solution was then placed into a refrigerator at 4°C and left to age overnight. During the aging process, the precipitate settles creating a clear phase separation. The HA precipitate was washed periodically in dH_2O whilst in storage to retain phase separation. Samples of the HA suspension were then aliquoted into 50mL tubes (FisherBrand) and centrifuged at 4000rpm for 5 minutes. The clear phase was removed and replaced with dH_2O. After resuspension in dH_2O, 3.7% hydrochloric acid (HCl) was added to adjust the pH to 7.5, followed by a final wash in dH_2O. Once neutralised, the centrifugation process was repeated until unbound water was negligible, creating a concentrated HA paste. The concentration of HA in the paste was measured by calculating the dry mass as a percentage of the initial sample mass. The dry mass was obtained by measuring a sample after baking at 80°C for 30 minutes. ***Bone Collagen/Hydroxyapatite Model:*** HA was added to 2.0mg/mL type-1 rat tail collagen in 0.1M acetic acid (First Link, UK) to the required concentration and mixed thoroughly. 10x MEM (Gibco) was added to this mixture and then neutralised using 5M and 1M NaOH until a colour change from yellow to pink was observed. TE85 hOS cells suspended in M1 were then added to the collagen solution and pipetted into a bespoke plastic O-ring (*ca.* 16mm internal diameter). The final solution comprised 85% collagen/HA solution, 10% 10x MEM and 5% cell suspension.

2.5 Co-culture Platform for 3D Tissue Engineered Skeletal Muscle and Bone Constructs.

3D co-culture moulds were created using Nunc Rectangular 8-well plates coated with PDMS. An area large enough to allow for the setting of the skeletal muscle construct and placement of the boundary was cut away from the PDMS covering the well, and a bespoke plastic O-ring was placed onto the remaining PDMS covering the well. 2.0mg/mL collagen was used to seal the resulting ring to the PDMS creating a well to set the bone construct in. A minutien pin was placed at the centre to act as an anchor point for the bone construct. A separate PDMS boundary was used to create the setting area for the skeletal muscle construct and sealed using 2.0mg/mL collagen (Figure 2).

Once the skeletal muscle and collagen/cell solutions were pipetted into the setting areas, the chamber was placed into a 37^{o}C humidified incubator and left until the collagen mixtures were fully polymerised. Once set, the construct was detached from the walls of the setting area, the PDMS and O-ring boundary wall removed and M1 added to the well, allowing the construct to float. Constructs were cultured for four days in M1, ensuring complete replacement of the medium twice daily. To induce cellular fusion, constructs were then cultured in MM for a further 10 days ensuring complete replacement of MM every 24 hours.

2.6 Cyto- and histochemistry

Fluorescent cell staining was performed as follows. Numbers in brackets represent timings used when working with 3D collagen scaffolds to enable liquid penetration through the matrix.

Following culture, the cells were washed twice with phosphate-buffered saline (PBS) and fixed by the drop wise addition of methanol and acetone (1:1 v/v) to PBS (50%

v/v). This was removed after 15 (30) minutes incubation and neat methanol and acetone (1:1 v/v) was added for a further 15 (30) minutes prior to staining.

Once fixed, cultures were stained for the muscle specific cytoskeletal intermediate filament desmin. Initially constructs were placed into a blocking solution consisting of 5% goat serum and 0.2% Triton X-100 in Tris-buffered saline (TBS) for 30 minutes (2 hours) and then incubated with rabbit anti-desmin antibody (Abcam, UK) for two hours (overnight) diluted 1:200 in 2% goat serum/TBS. The cells were then incubated in the dark for a further two hours in goat anti-rabbit IgG Rhodamine-derived tetramethylrhodamine (TRITC) or Chromeo 488 conjugated secondary antibody (Abcam) diluted 1:200 in TBS. For indirect contact monolayer cultures, Phalloidin conjugated with the fluorescent dye Rhodamine was used to visualise cytoskeletal F-actin (Life Technologies). Samples were incubated in a 1:200 solution of Rhodamine Phalloidin with 0.1% Triton-X in PBS for 30 minutes.

DAPI was used as a counterstain to observe cell nuclei. Samples were incubated in a 1:10,000 dilution (1mg/mL, Thermo Scientific Pierce) in dH_2O for 15 (30) minutes in the dark before being washed at least five times in dH_2O. All samples were mounted on glass microscope slides using Fluoromount Aqueous Mounting Medium (Sigma) and imaged using a Leica DM2500 fluorescence microscope with associated software.

2.7 RNA extraction and Quantitative Reverse Transcription Polymerised Chain Reaction

Monolayer samples used for qRT-PCR analysis were first lysed in 500µL TRI-reagent (Fisher). 3D cultures were placed into 500µL TRI reagent and snap frozen in liquid nitrogen. Samples were then stored at -80^{o}C for later RNA extraction.

Prior to RNA extraction, samples were thawed at room temperature. A steel ball bearing was added to 3D construct samples and then agitated on a TissueLyser II (Qiagen) for 4 minutes at 10,000rpm to ensure homogenisation and cell lysis. RNA was extracted using TRI-Reagent® (Sigma) according to manufacturer's guidelines. qRT-PCR reactions were performed using QuantiFast SYBR Green RT-PCR kit (Qiagen) and primers (Table 2) with cycling as follows: 50°C for 10 minutes (reverse transcription/cDNA synthesis), 95°C for 5 minutes (transcriptase inactivation and initial denaturation step) followed by PCR steps for 40 cycles; 95°C for 10 seconds (denaturation), 60°C for 30 seconds (annealing and elongation). Finally, a dissociation/melt curve analysis was performed to allow exclusion of non-specific amplification or primer-dimer interference. Relative gene expression was calculated using ΔΔCT equation [48] where relative expression is calculated as $2^{-\Delta\Delta CT}$ (Fold Change). Each individual sample was assessed in triplicate and normalised to a single designated POLR2B reference gene.

2.8 Alkaline Phosphatase Activity, DNA and Protein Quantification

Monolayer samples taken for Alkaline Phosphatase (ALP), DNA and protein analysis were lysed in dH_2O and taken through 3 freeze-thaw cycles. 3D tissue engineered samples were snap frozen with 500µL of dH_2O in liquid nitrogen. Samples were stored at -80°C for later use. A steel ball bearing was added to 3D construct samples and then agitated on a TissueLyser II (Qiagen) for 4 minutes at 10,000rpm. For studies not involving direct contact with HA, DNA content was measured using a NanoDrop™ 2000 spectrophotometer at 260nm (Thermo Scientific). For studies involving direct contact with HA, commercially available Quant-iT™ PicoGreen dsDNA Kits (Invitrogen) were used according to manufacturer's guidelines.

ALP was measured using a 4-methylumbelliferyl phosphate (MUP) de-phosphorylation assay in which 50µl of the cell/lysis buffer solution was placed into a 96-well plate with 50µl of dH_2O. To this 50µl of 4-MUP was added and left for 30 minutes. To stop the reaction, 50µl of 100mM ethylenediaminetetraacetic acid (EDTA) buffer was added. Absorbance readings taken using a Varioskan Flash (ThermoScientific) at 440nm. Results were compared with a standard curve of 4-MU. ALP was normalised to DNA for later construct configuration comparison. Protein concentrations were measured using a NanoDrop™ 2000 spectrophotometer at 280nm [49].

2.9 Metabolic Activity per Live Cell and Membrane Integrity Measurements

Metabolic activity was measured using a 10% (v/v) solution of PrestoBlue (Invitrogen) in the respective growth medium. Cells were incubated for 30 minutes in culture conditions and then 100µL sampled and read at 544nm/590mn (excitation/emission) using a Varioskan Flash. Following trypsinization, membrane integrity (viability) and live cell numbers were measured using an Acridine Orange (30 µg/mL)/DAPI (100 µg/mL) solution and image analysis on Nucleocounter NC-3000 (Chemometec).

2.10 Myotube characteristics

Mean number of myotubes, fusion index (percentage of nuclei attributed to myotubes) and mean number of nuclei per myotube were measured manually from fluorescent images using ImageJ (NIH).

2.11 Statistics

All data are presented as mean ± standard deviation. To determine if statistical differences existed between different medium compositions or indirect co-cultures,

ANOVAs were performed with a Bonferroni post-hoc test. The results of the 3D TE co-cultures were analysed using a two-tailed t-test. All statistical analyses were conducted using GraphPad Prism 5.0.

3 Results

3.1 Medium Composition Culture Comparisons

To create a system in which the major musculoskeletal components of skeletal muscle and bone can be co-cultured in 3D, a medium must first be identified that can sustain the growth and differentiation of both cell types. Three proliferation phase media were tested; followed by differentiation phase analysis using a myogenic and an osteogenic medium (Table 1). DNA concentration changes were used as an indicator of population change and protein/DNA ratios as an indicator of cell size.

3.1.1 Proliferation Phase

After 48 hours, both C2C12 and TE85 DNA and protein (Figure 3A-D) concentrations increased without any significant differences occurring between the three growth media. After 96 hours, C2C12s grown in M1 (C2C12 control medium) had significantly greater DNA and protein concentrations than those cultured in M2 and M3 ($p \leq 0.001$), demonstrating greater proliferation in this control media. Contrastingly, TE85s cultured in M2 (TE85 control medium) had significantly greater DNA and protein concentrations than either M1 or M3 at 96 hours ($p \leq 0.001$). TE85s cultured in M3 exhibited reduced concentrations of DNA and protein compared to both M1 and M2 respectively, therefore, to achieve a consistent proliferation timeline comparative to previous cultures and models, M3 would be unsuitable for co-culture. These trends can also be observed in brightfield images (Supplementary Figure 1) with increasing coverage to full confluency for all conditions after 96 hours, except for TE85s cultured in M3, which

show large areas of uncovered surface. Protein/DNA (Figure 3E, F) ratios indicate changes in cellular population morphology. After 96 hours, no significant differences occur between M1, M2 or M3 conditions in both C2C12 and TE85 cultures.

This data indicates that each medium condition produced only a proliferative effect rather than additional changes in cell size (hyperplasia rather than hypo- or hypertrophy), although a numerical bias towards the control media was observed. This bias was more pronounced without a preconditioning step, where changes in basal medium (from DMEM to EMEM or EMEM to DMEM) resulted in significantly less ($P<0.001$) DNA concentrations at 96 hours after seeding (Supplementary Figure 1).

Additionally, for C2C12s cultured in M1, metabolic activity per live cell (MAC) was slightly greater, although not statistically significant (Figure 3G, H). Conversely, for TE85s, M1 cultures exhibited a slightly lower non-significant MAC, potentially reflecting the lower 96h DNA profile than M2 culture despite non-significance after 48 hours. Membrane integrity (Figure 3 I, J), following passage at 96h, was not significantly different in C2C12s (*ca.*93%). In TE85 M1 cultures, membrane integrity was statistically significantly lower, although this difference is considered negligible (*ca.*96.0 ± 1.0% vs *ca.*98.0 ± 0.4%).

Although TE85s cultured in M2 demonstrated significantly greater DNA concentrations after 96 hours, TE85 M1 cultures were still able to reach full confluency, whilst M2 affected C2C12 cultures to a greater extent than M1 (C2C12 control medium), possibly due to the reduced serum (20% in M1, 10% in M2). Following this, M1 was chosen as a proliferation medium for subsequent medium composition and co-culture experiments.

3.1.2 Differentiation Phase

Fluorescent microscopy shows C2C12s cultured in MM have successfully formed myotubes and become increasingly hypertrophic at 72 hours, with some unassociated nuclei present (Figure 4A-F). Corresponding DNA concentrations did not significantly change over the 72 hour differentiation period indicating exit from the cell cycle. This is accompanied by a significant ($p<0.01$) increase in protein/DNA ratios after 48hrs (Figure 4P-Q). C2C12s in OM experienced a significant reduction ($p<0.0001$) in DNA concentrations after 48 hours. This was without an accompanying change in protein/DNA ratios, indicating a loss in cell number, possibly due to detachment through over-confluence. However, these cultures still had greater DNA concentrations than C2C12s (MM) after 72 hours. C2C12s in OM also experienced a reduction in desmin presence over the culture period indicating a probable loss of myogenic potential.

TE85 cultures in OM show a greater concentration ($p<0.05$) of DNA after 24 hours in comparison to MM, although only M2+OM (TE85 control medium) had significantly greater DNA after 72 hours ($p<0.05$). Brightfield micrographs support this with an observable increase in cell density over time in OM cultures (Figure 4: H-K-N and I-L-O) without cell size changes occurring (due to potentially harmful factors such as aging) as indicated by protein/DNA ratios not varying significantly over time (Figure 4T-U).

qRT-PCR results of C2C12 myogenin expression (Figure 4R) showed an increase over 72 hours in MM, with no changes evident within OM. To confirm no osteogenic effects within the C2C12 population, RUNX2 expression was also assessed (Figure 4S) and no significant changes were observed. RUNX2 expression within TE85 cultures increased significantly in all cultures (Figure 4V). Fluorescent imaging in TE85 cultures showed no

desmin presence across all cultures indicating no lineage altering effects of MM (Supplementary Figure S2).

With a reduction in desmin presence and no myogenic fusion, in addition to the lack of change in myogenin expression in C2C12 OM cultures as well as an increase in RUNX2 in TE85 MM cultures, M1 followed by MM has demonstrated a suitability to enable the development of a skeletal muscle and bone co-culture system.

3.2 Effects of Indirect Contact of Skeletal Muscle and Bone in Monolayer Cultures

As a monolayer representation of 3D skeletal muscle and bone cultures, monolayer cultures of C2C12 and TE85/HA were co-cultured in the same well but separated by a PDMS boundary. This was to understand the effects of TE85 and C2C12 inter-cellular interactions, such as paracrine signalling, and contact with HA.

Unlike the C2C12 fusion to form myotubes, TE85s do not visibly differentiate. To differentiate, cells must first exit the cell cycle, so to assess changes in TE85 cell growth, DNA concentrations were measured after direct/no exposure to HA and with/without C2C12s cultured in the adjacent chamber. TE85's co-cultured with C2C12's in the absence of HA had significantly greater DNA concentrations than all other conditions (Figure 5A). This indicates that the addition of secreted factors from the C2C12s are influencing the growth of the TE85s in co-culture. These factors would not be present in TE85 only cultures and the influence may be reduced by the presence of HA in the TE85/C2C12+HA cultures. ALP concentrations of TE85 cultures normalised to DNA (Figure 5B), shows that the addition of C2C12 and HA does not inhibit production of ALP relative to TE85 only controls and is significantly greater ($p \leq 0.05$) than C2C12/TE85-HA cultures.

Immunofluorescence of C2C12 cultures (Figure 5C-F) shows evidence of myogenic fusion in all cultures although C2C12/TE85+HA cultures appear to show reduced myotube formation. Although desmin is still present in the non-fused cells. Image analysis (Figure 5G-I) confirms that fusion is limited in C2C12s with both the presence of TE85s and HA, although not in HA conditioned medium. This suggests that TE85s paracrine and secreted factors reduce the fusion capability of C2C12s in the culture timeframe, the effect of which is enhanced with an interaction with HA.

3.3 Co-culture of Tissue Engineered 3D Skeletal Muscle and Bone Constructs

Prior to the creation of a musculoskeletal junction, conditions amenable to the successful co-culture of skeletal muscle and bone must first be understood. 3D Skeletal muscle and bone cultures were set up and cultured in the same well. After 14 days culture (4 days M1, 10 days MM) samples were taken to analyse markers of differentiation. RUNX2/CBFa1 mRNA expression was induced nearly 150-fold ($p<0.05$) in bone constructs co-cultured alongside engineered skeletal muscle in comparison to bone constructs cultured in isolation in the same media conditions (Figure 6A). Osteocalcin/BGLAP (Figure 6B) was also found to be more highly expressed ($p\leq0.05$) in co-cultures. ALP concentration was not significantly different between cultures although co-culture levels tended to be lower (Figure 6C). These results indicate that co-culture bone cell populations exhibit a greater osteogenic potential than control cultures, and also demonstrates that C2C12s positively interact with TE85 cultures in 3D. The presence of HA in the scaffold precluded the use of common stains, such as Alizarin Red, and obscures observation of the cells through brightfield microscopy, as such further analysis through microscopy could not be obtained.

Cellular fusion was observed in all constructs (Figure 6D-F) although in the co-cultured skeletal muscle construct there were large numbers of unfused cells and the existing myotubes were not as hypertrophic as those in the skeletal muscle constructs cultured in isolation. Mean maximum myotube length per image reflects this with skeletal muscle only cultures demonstrating a significantly greater ($p \leq 0.05$) mean maximum length; although the mean length for both skeletal muscle only and co-cultures were not significantly different. However, the average number of myotubes per image was substantially reduced in co-culture constructs ($p < 0.001$). This demonstrates a continuation of the negative effects shown in monolayer cultures in the reduction in myotube formation.

4 Discussion

Successful development of a skeletal muscle and bone co-culture, which replicates key characteristics of *in vivo* tissue, would be of great benefit to *in vitro* investigations into the musculoskeletal system and could enable the progress towards the generation of a full *in vitro* musculoskeletal junction (muscle-tendon-bone). Progression of such a culture system with standardised manufacturing parameters, such as those proposed by Wragg [50,51], could also reduce the reliance on animal models in pre-clinical studies, whilst also allowing for the testing of efficacy and toxicity of developmental pharmaceuticals, biomaterials and medical devices in a more biomimetic environment. In the present study, the variables required to facilitate co-culture of both the C2C12 myogenic and TE85 osteogenic cell lines have been established, culminating in successful growth and differentiation of skeletal muscle and bone 3D tissues *in vitro*.

As one of the major factors affecting myoblast fusion and bone matrix secretion, investigating the effects of different medium composition on proliferation and

differentiation is of high importance. Whilst co-culture systems described within the literature report the influence of one cell type on the other, these papers have yet to describe the conditions which allow for the successful culture and differentiation of both cell types in a single medium system through experimental comparisons [52–55].

In the experiments reported herein, a restriction in the concentrations of glucose between medium significantly negatively affected the C2C12 line and was not offset by the addition of glutamine [56–58]. A deficit in the FBS supplement concentration was also implicated in the restriction of population growth of the myogenic cells. Myogenic cell lineages are typically cultured in a high glucose (4500 mg/L) basal medium with at least 10% foetal bovine serum (FBS) although 20% FBS supplementation has been shown to produce more favourable results [59–63]. Conversely, the TE85 cell line showed greater proliferation with a lower glutamine, glucose and FBS concentrations. Osteogenic cell lineages are typically cultured in low glucose (1000 mg/L) medium with 10% FBS and an addition of non-essential amino acids [64–68]. Regardless of these outcomes, both skeletal muscle and osteoblast-like cell types show a capacity for proliferation in all media with a bias towards each cell type's typical culture medium as expected. However, C2C12s were affected to a greater extent than TE85's resulting in high-glucose DMEM + 20% FBS being chosen as a suitable proliferation medium for both cell lines.

Myogenic cells have also shown the ability to differentiate along an osteoblastic lineage and conditions promoted through blast and crush injury demonstrate this capacity *in vivo* [69][59,69–72]. As a marker for osteoblast progression, RUNX2 has been established as the initial trigger of the osteogenic cascade resulting in ALP production and an upregulation of BGLAP/Osteocalcin. Under culture

with common osteogenic supplement's (β-glycerol-phosphate, ascorbic acid and dexamethasone), C2C12s showed no change in myogenin expression across three days and no significant differences in RUNX2 expression. This is in comparison to the classic upregulation followed by subsequent decrease in myogenin expression observed in MM serum-starved cultures [42,73–75]. Under reduced serum conditions (MM), C2C12s fused to form small myotubes dispersed between desmin positive cells, which later progressed to form multiple hypertrophic myotubes, in line with classic *in vitro* skeletal muscle culture. However, C2C12s cultured in OM demonstrated a decrease in desmin presence with an increase in non-desmin associated nuclei and punctate staining. The low glucose aspect of the OM potentially caused a reduction in metabolic activity, accompanied by the presence of dexamethasone, a known inducer of atrophy [76–78] and other osteogenic factors, may have caused a reversion to a more progenitor-like state, alluded to in skeletal muscle calcification conditions [69]. A lack of RUNX2/Cbfa1 up-regulation supports a reversion theory to a less committed cell type, rather than a direct lineage change as in the case of BMP-2 stimulated culture [59].

Much like the skeletal MPCs, osteoblasts exit the cell cycle prior to differentiating [79,80]. Once the TE85 cultures growth profiles are stabilised, they displayed an up-regulation of RUNX2/Cbfa1 in all cultures after 3 days and no desmin associated nuclei without evidence of cellular fusion. The concentration and the type of serum in the differentiation medium do not seem to affect the final expression of RUNX2/CBFa1. However, the osteogenic supplements may reduce the latent time before expression is upregulated. Therefore, low non-foetal serum (2% horse serum) could be used in subsequent studies involving osteoblasts-like cells, which would reduce the costs involved in cultures of this type.

Once defining the appropriate medium compatibility protocol, the influence of each cell type in the same culture environment was assessed with the addition of HA to stimulate further differentiation and mimic part of the composition of *in vivo* bone matrix. HA, in this case, was found to inhibit DNA concentrations within TE85 populations in co-culture with C2C12s but increase ALP/DNA in TE85 only and co-culture conditions. TE85s may have down regulated markers relevant to the production of ALP and are therefore self-regulating responses once exposed to HA. This self-regulation has been reported in reference to organic/inorganic pyrophosphate ratios [81].

Current monolayer toxicity tests are generally single cell type and conducted in accordance with ISO10993 for medicinal devices or through HTS in drug discovery (ISO Identification of Medicinal Products). The monolayer system presented here, using both skeletal muscle and osteoblast cell lines, and incorporating elements of ECM to induce osteogenesis, creates a more relevant system for testing neighbourhood effects of toxicity. The ease of setup would lend itself to high-throughput techniques in smaller culture wells, although alternatives, such as trans-well inserts should be considered [82–85]. Additionally, this system could be used to investigate musculoskeletal conditions, such as the exposure of skeletal muscle to bone cells and ECM in blast injuries [69] by removal of the central barrier, similar to Wang et al. [86], in which mature populations were allowed to migrate and mix when observing enthesis healing.

The final component of the 3D co-culture, the collagen scaffold, allows the cells to reside in three dimensions. Reported medium protocols do not normally change between monolayer and 3D work, however, 3D cultures exhibit longer culture periods before definitive differentiation [16,23,87]. Additionally, considering the different volumetric shapes and mechanical influences (anchor points) to which each of the skeletal muscle

and bone construct were developed, a novel co-culture system needed to be created to allow co-exposure to the medium. Previous co-culture systems utilised a well-established delamination model, creating cylindrical 3D constructs and concentrating on biological outputs without regard to creating individual properties to best support each tissues formation [88–90]. The platform developed here sought to enable the formation of each of the constructs as previously described, in both shape and cellular differentiation [5,11,16,50]. Subsequent observation of each construct did not demonstrate any obvious deviation from single construct formation and analysis of differentiation showed enhancement of gene expression in the bone construct. Whilst fusion in the skeletal muscle constructs was diminished, an increased culture period may encourage similar myotube characteristics to isolated skeletal muscle constructs to be obtained. This diminished myotube fusion in the presence of HA and TE85s was also observed in the monolayer co-cultures and indicates continuity in cell behaviour between monolayer and 3D platforms. Increasing bone specific gene expression in the presence of skeletal muscle, without mechanical loading, is supported by a growing body of work in the influence of "myokines" on bone formation [91–93]. The effect of bone on muscle has had little study, although it has been reported that bone cell culture secretions impair skeletal muscle formation [94].

Considering the reported successes in skeletal muscle-tendon and bone-tendon models, [88,90] as well as tendon formation in a collagen hydrogel, the addition of a tendon component to this model should not be considered a prohibitive obstacle to the construction of an *in vitro* musculoskeletal junction [95,96]. Ultimately, this strategy can be applied to more physiologically relevant human stem cell-derived cell types involved

in the native musculoskeletal junction in order to achieve a more accurate prediction of drug testing responses.

In summary, this study represents the first reported instance of simultaneous 3D tissue engineered skeletal muscle and bone differentiation in co-culture, with evidence of an enhancing effect on bone specific gene expression. A single growth medium (high glucose DMEM + 20% FBS) was found to enable proliferation of the C2C12 muscle precursor and the TE85 osteosarcoma cell lines. This was coupled with high glucose DMEM+2% horse serum to enable fusion of C2C12s to form myotubes, an increase in expression of RUNX2/CBFa1 in TE85 cultures. When in monolayer co-culture, both cell types could proliferate and differentiate in the presence of each other and hydroxyapatite with the chosen medium protocol. 3D co-culture of skeletal muscle and bone *in vitro* demonstrated enhanced osteogenic gene expression in the bone model, in comparison to isolated bone controls, with no significant differences in ALP activity. Co-cultured skeletal muscle constructs retained a capacity for myoblast fusion, though this appeared diminished when compared to controls.

Future work should seek to use the methods described here to create a 3D tendon construct with a view to attachment to the bone and skeletal muscle models to form a full *in vitro* 3D tissue engineered musculoskeletal junction (muscle-tendon-bone). Additionally, the monolayer co-culture model should be further characterised in conjunction with the 3D co-culture to enable a comparative platform progression for testing.

Acknowledgements

Funding from the Doctoral Training Centre of Regenerative Medicine, (EPSRC, UK) is gratefully acknowledged.

Conflict of interest

The authors declare no financial or commercial conflict of interest.

5 References

[1] Nam, K.-H., Smith, A. S. T., Lone, S., Kwon, S., Kim, D.-H., Biomimetic 3D Tissue Models for Advanced High-Throughput Drug Screening. *J. Lab. Autom.* 2015, *20*, 201–215.

[2] Vandenburgh, H., Shansky, J., Benesch-Lee, F., Barbata, V., Reid, J., et al., Drug-screening platform based on the contractility of tissue-engineered muscle. *Muscle Nerve* 2008, *37*, 438–447.

[3] Eschenhagen, T., Zimmermann, W. H., Engineering Myocardial Tissue. *Circ. Res.* 2005, *97*, 1220–1231.

[4] Smalley, K. S., Lioni, M., Noma, K., Haass, N. K., Herlyn, M., In vitro three-dimensional tumor microenvironment models for anticancer drug discovery. *Expert Opin. Drug Discov.* 2008, *3*, 1–10.

[5] Smith, A. S. T., Passey, S., Greensmith, L., Mudera, V., Lewis, M. P., Characterization and optimization of a simple, repeatable system for the long term in vitro culture of aligned myotubes in 3D. *J. Cell. Biochem.* 2012, *113*, 1044–53.

[6] Mulhall, H. J., Hughes, M. P., Kazmi, B., Lewis, M. P., Labeed, F. H., Epithelial cancer cells exhibit different electrical properties when cultured in 2D and 3D environments. *Biochim. Biophys. Acta* 2013, *1830*, 5136–41.

[7] Mobasheri, A., Lewis, M., Tissue Engineered Animal Sparing Models for the Study of Joint and Muscle Diseases. in: Andrades, J. A. (Ed.), *Regenerative Medicine and Tissue Engineering*, InTech, 2013, pp. 509–541.

[8] Langley, G., The validity of animal experiments in medical research. *RSDA* 2009, *1*, 161–168.

[9] Elliott, N. T., Yuan, F., A Review of Three-Dimensional In Vitro Tissue Models for Drug Discovery and Transport Studies. *J. Pharm. Sci.* 2011, *100*, 59–74.

[10] Juhas, M., Engelmayr, G. C., Fontanella, A. N., Palmer, G. M., Bursac, N., Biomimetic engineered muscle with capacity for vascular integration and functional maturation in vivo. *Proc. Natl. Acad. Sci. U. S. A.* 2014, *111*, 5508–13.

[11] Sharples, A. P., Player, D. J., Martin, N. R. W., Mudera, V., Stewart, C. E., et al., Modelling in vivo skeletal muscle ageing in vitro using three-dimensional bioengineered constructs. *Aging Cell* 2012, *11*, 986–95.

[12] Sundelacruz, S., Li, C., Choi, Y. J., Levin, M., Kaplan, D. L., Bioelectric modulation of wound healing in a 3D invitro model of tissue-engineered bone. *Biomaterials* 2013, *34*, 6695–6705.

[13] Choi, S. H., Chung, K. Y., Johnson, B. J., Go, G. W., Kim, K. H., et al., Co-culture of bovine muscle satellite cells with preadipocytes increases PPARγ and C/EBPβ gene expression in differentiated myoblasts and increases GPR43 gene expression in adipocytes. *J. Nutr. Biochem.* 2013, *24*, 539–543.

[14] Fujita, H., Endo, A., Shimizu, K., Nagamori, E., Evaluation of serum-free differentiation conditions for C2C12 myoblast cells assessed as to active tension generation capability. *Biotechnol. Bioeng.* 2010, *107*, 894–901.

[15] Hinds, S., Tyhovych, N., Sistrunk, C., Terracio, L., Improved tissue culture conditions for engineered skeletal muscle sheets. *ScientificWorldJournal.* 2013, *2013*, 370151.

[16] Player, D. J., Martin, N. R. W., Passey, S. L., Sharples, a P., Mudera, V., et al., Acute mechanical overload increases IGF-I and MMP-9 mRNA in 3D tissue-engineered skeletal muscle. *Biotechnol. Lett.* 2014, *36*, 1113–24.

[17] Martin, N. R. W., Turner, M. C., Farrington, R., Player, D. J., Lewis, M. P., Leucine elicits myotube hypertrophy and enhances maximal contractile force in tissue engineered skeletal muscle in vitro. *J. Cell. Physiol.* 2017, *232*, 2788–2797.

[18] Huang, Y., Dennis, R. G., Larkin, L., Baar, K., Rapid formation of functional muscle in vitro using fibrin gels. *J Appl Physiol* 2005, *98*, 706–713.

[19] Neidlinger-Wilke, C., Grood, E. S., Wang JH-C, Brand, R. a, Claes, L., Cell alignment is induced by cyclic changes in cell length: studies of cells grown in cyclically stretched substrates. *J. Orthop. Res.* 2001, *19*, 286–93.

[20] Dennis, R. G., Kosnik, P. E., Excitability and isometric contractile properties of mammalian skeletal muscle constructs engineered in vitro. *In Vitro Cell. Dev. Biol. Anim.* 2000, *36*, 327–335.

[21] Powell, C. A., Smiley, B. L., Mills, J., Vandenburgh, H. H., Mechanical stimulation improves tissue-engineered human skeletal muscle. *Am. J. Physiol. Cell Physiol.* 2002, *283*, C1557-65.

[22] Mudera, V., Smith, A. S. T., Brady, M. A., Lewis, M. P., The effect of cell density on the maturation and contractile ability of muscle derived cells in a 3D tissue-engineered

skeletal muscle model and determination of the cellular and mechanical stimuli required for the synthesis of a postural phenotype. *J. Cell. Physiol.* 2010, *225*, 646–53.

[23] Martin, N. R. W., Passey, S. L., Player, D. J., Khodabukus, A., Ferguson, R. a, et al., Factors affecting the structure and maturation of human tissue engineered skeletal muscle. *Biomaterials* 2013, *34*, 5759–65.

[24] Boonen, K. J. M., Langelaan, M. L. P., Polak, R. B., van der Schaft, D. W. J., Baaijens, F. P. T., et al., Effects of a combined mechanical stimulation protocol: Value for skeletal muscle tissue engineering. *J. Biomech.* 2010, *43*, 1514–1521.

[25] Hinds, S., Bian, W., Dennis, R. G., Bursac, N., The role of extracellular matrix composition in structure and function of bioengineered skeletal muscle. *Biomaterials* 2011, *32*, 3575–3583.

[26] Eastwood, M., Mudera, V. C., Mcgrouther, D. A., Brown, R. A., Effect of precise mechanical loading on fibroblast populated collagen lattices: Morphological changes. *Cell Motil. Cytoskeleton* 1998, *40*, 13–21.

[27] Laurencin, C. T., Ambrosio, a M., Borden, M. D., Cooper, J. a, Tissue engineering: orthopedic applications. *Annu. Rev. Biomed. Eng.* 1999, *1*, 19–46.

[28] Brown, J. L., Kumbar, S. G., Laurencin, C. T., Bone Tissue Engineering. *Bone Tissue Engineering*, Elsevier, 2013.

[29] Syed-Picard, F. N., Larkin, L. M., Shaw, C. M., Arruda, E. M., Three-dimensional engineered bone from bone marrow stromal cells and their autogenous extracellular matrix. *Tissue Eng. Part A* 2009, *15*, 187–195.

[30] Kamath, M. S., Ahmed, S. S. S. J., Dhanasekaran, M., Santosh, S. W., Bone Regeneration Based on Tissue Engineering Conceptions – A 21st Century Perspective. *Int. J. Nanomedicine* 2014, *9*, 183–95.

[31] Cheng, C. W., Solorio, L. D., Alsberg, E., Decellularized tissue and cell-derived extracellular matrices as scaffolds for orthopaedic tissue engineering. *Biotechnol. Adv.* 2014, *32*, 462–484.

[32] Petite, H., Viateau, V., Bensaïd, W., Meunier, A., de Pollak, C., et al., Tissue-engineered bone regeneration. *Nat. Biotechnol.* 2000, *18*, 959–63.

[33] Boskey, A. L., Natural and Synthetic Hydroxyapatites. *Natural and Synthetic*

Hydroxyapatites, Elsevier, 2013.

[34] Hench, L. L., Best, S. M., Ceramics, Glasses, and Glass-Ceramics. *Ceramics, Glasses, and Glass-Ceramics*, Elsevier, 2013.

[35] Gentile, P., Chiono, V., Carmagnola, I., Hatton, P. V, An overview of poly(lactic-co-glycolic) acid (PLGA)-based biomaterials for bone tissue engineering. *Int. J. Mol. Sci.* 2014, *15*, 3640–59.

[36] Lou, T., Wang, X., Song, G., Structure and properties of PLLA / b -TCP nanocomposite scaffolds for bone tissue engineering. *J Mater Sci Mater Med* 2015, *26*, DOI 10.1007/s10856-014-5366-2.

[37] Padmanabhan, S. K., Sannino, A., Licciulli, A., Preparation and characterization of Collagen / hydroxyapatite microsphere composite scaffold for bone regeneration. 2014, *587*, 239–244.

[38] Murugan, R., Ramakrishna, S., Nano-featured scaffolds for tissue engineering: a review of spinning methodologies. *Tissue Eng.* 2006, *12*, 435–47.

[39] Kim, Y. B., Kim, G. H., PCL/Alginate Composite Sca ff olds for Hard Tissue Engineering: Fabrication, Characterization, and Cellular Activities. *ACS Comb. Sci.* 2014, DOI 10.1021/co500033h.

[40] Henson, F., Getgood, A., The use of scaffolds in musculoskeletal tissue engineering. *Open Orthop. J.* 2011, *5 Suppl 2*, 261–6.

[41] Oryan, A., Alidadi, S., Moshiri, A., Maffulli, N., Bone regenerative medicine: classic options, novel strategies, and future directions. *J. Orthop. Surg. Res.* 2014, *9*, 18.

[42] Langenbach, F., Handschel, J., Effects of dexamethasone, ascorbic acid and β-glycerophosphate on the osteogenic differentiation of stem cells in vitro. *Stem Cell Res. Ther.* 2013, *4*, 117.

[43] Wimpenny, I., Hampson, K., Yang, Y., Ashammakhi, N., Forsyth, N. R., One-step recovery of marrow stromal cells on nanofibers. *Tissue Eng. Part C. Methods* 2010, *16*, 503–9.

[44] Bölgen, N., Yang, Y., Korkusuz, P., Güzel, E., El Haj, A. J., et al., Three-dimensional ingrowth of bone cells within biodegradable cryogel scaffolds in bioreactors at different regimes. *Tissue Eng. Part A* 2008, *14*, 1743–50.

[45] Heinemann, C., Heinemann, S., Worch, H., Hanke, T., Development of an

osteoblast/osteoclast co-culture derived by human bone marrow stromal cells and human monocytes for biomaterials testing. *Eur. Cell. Mater.* 2011, *21*, 80–93.

[46] Cheng, H., Jiang, W., Phillips, F. M., Haydon, R. C., Peng, Y., et al., Osteogenic activity of the fourteen types of human bone morphogenetic proteins (BMPs). *J. Bone Joint Surg. Am.* 2003, *85-A*, 1544–52.

[47] Liu, Y., Williams, D. J., Incorporation of Hydroxyapatite Sol Into Collagen Gel to Regulate the Contraction Mediated by Human Bone Marrow-Derived Stromal Cells. *IEEE Trans. Nanobioscience* 2010, *9*, 1–11.

[48] Livak, K. J., Schmittgen, T. D., Analysis of Relative Gene Expression Data Using Real-Time Quantitative PCR and the 2−ΔΔCT Method. *Methods* 2001, *25*, 402–408.

[49] Desjardins, P., Hansen, J. B., Allen, M., Microvolume Protein Concentration Determination Using the NanoDrop 2000c Spectrophotometer. *J. Vis. Exp.* 2009, DOI 10.3791/1610.

[50] Wragg, N. M., Development of a 3D Tissue Engineered Skeletal Muscle and Bone Pre-Clinical Co-Culture Platform [Thesis]. Loughborough University, 2016.

[51] Wragg, N. M., Player, D. J., Martin, N. R. W., Liu, Y., Lewis, M. P., Development of tissue - engineered skeletal muscle manufacturing variables. *Biotechnol. Bioeng.* 2019, 1–13.

[52] Mikos, A. G., Herring, S. W., Ochareon, P., Lu, H. H., Kandel, R., et al., Engineering Complex Tissues. *Tissue Eng.* 2006, *12*, 3307.

[53] Eckle, V.-S., Drexler, B., Grasshoff, C., Seeger, T., Thiermann, H., et al., Spinal cord - skeletal muscle cocultures detect muscle-relaxant action of botulinum neurotoxin A. *ALTEX* 2014, 433–440.

[54] Kino-oka, M., Kim, J., Kurisaka, K., Kim, M.-H., Preferential growth of skeletal myoblasts and fibroblasts in co-culture on a dendrimer-immobilized surface. *J. Biosci. Bioeng.* 2013, *115*, 96–99.

[55] Kulesza, A., Burdzinska, A., Szczepanska, I., Zarychta-Wisniewska, W., Pajak, B., et al., The mutual interactions between mesenchymal stem cells and myoblasts in an autologous co-culture model. *PLoS One* 2016, *11*, 1–19.

[56] Behjousiar, A., Kontoravdi, C., Polizzi, K. M., In situ monitoring of intracellular glucose and glutamine in CHO cell culture. *PLoS One* 2012, *7*, 1–9.

[57] Lu, F., Toh, P. C., Burnett, I., Li, F., Hudson, T., et al., Automated dynamic fed-batch process

and media optimization for high productivity cell culture process development. *Biotechnol. Bioeng.* 2013, *110*, 191–205.

[58] Yuneva, M., Zamboni, N., Oefner, P., Sachidanandam, R., Lazebnik, Y., Deficiency in glutamine but not glucose induces MYC-dependent apoptosis in human cells. *J. Cell Biol.* 2007, *178*, 93–105.

[59] Katagiri, T., Yamaguchi, A., Komaki, M., Abe, E., Takahashi, N., et al., Bone morphogenetic protein-2 converts the differentiation pathway of C2C12 myoblasts into the osteoblast lineage. *J. Cell Biol.* 1994, *127*, 1755–1766.

[60] Cooper, S. T., Maxwell, a L., Kizana, E., Ghoddusi, M., Hardeman, E. C., et al., C2C12 co-culture on a fibroblast substratum enables sustained survival of contractile, highly differentiated myotubes with peripheral nuclei and adult fast myosin expression. *Cell Motil. Cytoskeleton* 2004, *58*, 200–11.

[61] Park, H., Bhalla, R., Saigal, R., Radisic, M., Watson, N., et al., Effects of electrical stimulation in C2C12 muscle constructs. *J. Tissue Eng. Regen. Med.* 2008, *2*, 279–287.

[62] Costantini, M., Testa, S., Mozetic, P., Barbetta, A., Fuoco, C., et al., Microfluidic-enhanced 3D bioprinting of aligned myoblast-laden hydrogels leads to functionally organized myofibers in vitro and in vivo. *Biomaterials* 2017, *131*, 98–110.

[63] Sharp, S. B., Kim, S., Lee, M., Sunday, L., Enriquez, E., et al., Culture of C2C12 and BC3H1 myogenic cells with iron-supplemented calf serum; rapid media screen. *Vitr. Cell. Dev. Biol. - Anim.* 1995, *31*, 749–751.

[64] San Martin, I. a, Varela, N., Gaete, M., Villegas, K., Osorio, M., et al., Impaired cell cycle regulation of the osteoblast-related heterodimeric transcription factor Runx2-Cbfbeta in osteosarcoma cells. *J. Cell. Physiol.* 2009, *221*, 560–71.

[65] Struewer, J., Roessler, P. P., Schuettler, K. F., Ruppert, V., Stein, T., et al., Influence of cyclical mechanical loading on osteogenic markers in an osteoblast-fibroblast co-culture in vitro: Tendon-to-bone interface in anterior cruciate ligament reconstruction. *Int. Orthop.* 2014, *38*, 1083–1089.

[66] Jones, G. L., Walton, R., Czernuszka, J., Griffiths, S. L., El Haj, A. J., et al., Primary human osteoblast culture on 3D porous collagen-hydroxyapatite scaffolds. *J. Biomed. Mater. Res. - Part A* 2010, *94*, 1244–1250.

[67] Gomes, M. E., Reis, R. L., Cunha, a M., Blitterswijk, C. a, de Bruijn, J. D., Cytocompatibility

and response of osteoblastic-like cells to starch-based polymers: effect of several additives and processing conditions. *Biomaterials* 2001, *22*, 1911–7.

[68] Wang, Z., Ma, Y., Wei, J., Chen, X., Cao, L., et al., Effects of sintering temperature on surface morphology/microstructure, in vitro degradability, mineralization and osteoblast response to magnesium phosphate as biomedical material. *Sci. Rep.* 2017, *7*, 823.

[69] Davies, O. G., Grover, L. M., Eisenstein, N., Lewis, M. P., Liu, Y., Identifying the Cellular Mechanisms Leading to Heterotopic Ossification. *Calcif. Tissue Int.* 2015, *97*, 432–444.

[70] Sinanan, A. C. M., Buxton, P. G., Lewis, M. P., Muscling in on stem cells. *Biol. Cell* 2006, *98*, 203–14.

[71] Mulhall, H., Patel, M., Alqahtani, K., Mason, C., Lewis, M. P., et al., Effect of capillary shear stress on recovery and osteogenic differentiation of muscle-derived precursor cell populations. *J. Tissue Eng. Regen. Med.* 2011, *5*, 629–635.

[72] Starkey, J. D., Yamamoto, M., Yamamoto, S., Goldhamer, D. J., Skeletal Muscle Satellite Cells Are Committed to Myogenesis and Do Not Spontaneously Adopt Nonmyogenic Fates. *J. Histochem. Cytochem.* 2011, *59*, 33–46.

[73] Maffulli, N., Leadbetter, W., Renstrèom, P., Tendon injuries : basic science and clinical medicine. *Tendon Injuries : Basic Science and Clinical Medicine*, 2005.

[74] Maegawa, N., Kawamura, K., Hirose, M., Yajima, H., Takakura, Y., et al., Enhancement of osteoblastic differentiation of mesenchymal stromal cells cultured by selective combination of bone morphogenetic protein-2 (BMP-2) and fibroblast growth factor-2 (FGF-2). *J. Tissue Eng. Regen. Med.* 2007, *1*, 306–313.

[75] Khatiwala, C. B., Kim, P. D., Peyton, S. R., Putnam, A. J., ECM compliance regulates osteogenesis by influencing MAPK signaling downstream of RhoA and ROCK. *J. Bone Miner. Res.* 2009, *24*, 886–98.

[76] Qin, J., Du, R., Yang, Y.-Q., Zhang, H.-Q., Li, Q., et al., Dexamethasone-induced skeletal muscle atrophy was associated with upregulation of myostatin promoter activity. *Res. Vet. Sci.* 2013, *94*, 84–9.

[77] Krug, A. A. L. O., Macedo, A. G., Zago, A. S., High-intensity resistance training attenuates dexamethasone-induced muscle atrophy High-intensity resistance training attenuates dexamethasone-induced muscle atrophy. 2012.

[78] Girón, M. D., Vílchez, J. D., Shreeram, S., Salto, R., Manzano, M., et al., β-Hydroxy-β-Methylbutyrate (HMB) Normalizes Dexamethasone-Induced Autophagy-Lysosomal Pathway in Skeletal Muscle. *PLoS One* 2015, *10*, e0117520.

[79] Funato, N., Ohtani, K., Ohyama, K., Kuroda, T., Nakamura, M., Common regulation of growth arrest and differentiation of osteoblasts by helix-loop-helix factors. *Mol. Cell. Biol.* 2001, *21*, 7416–7428.

[80] Gaur, T., Lengner, C. J., Hovhannisyan, H., Bhat, R. a., Bodine, P. V. N., et al., Canonical WNT signaling promotes osteogenesis by directly stimulating Runx2 gene expression. *J. Biol. Chem.* 2005, *280*, 33132–33140.

[81] Golub, E. E., Harrison, G., Taylor, a G., Camper, S., Shapiro, I. M., The role of alkaline phosphatase in cartilage mineralization. *Bone Miner.* 1992, *17*, 273–278.

[82] Takegahara, Y., Yamanouchi, K., Nakamura, K., Nakano, S., Nishihara, M., Myotube formation is affected by adipogenic lineage cells in a cell-to-cell contact-independent manner. *Exp. Cell Res.* 2014, *324*, 105–14.

[83] Dines, J. S., Grande, D. a., Dines, D. M., Tissue engineering and rotator cuff tendon healing. *J. Shoulder Elb. Surg.* 2007, *16*, 204–207.

[84] Miki, Y., Ono, K., Hata, S., Suzuki, T., Kumamoto, H., et al., The advantages of co-culture over mono cell culture in simulating in vivo environment. *J. Steroid Biochem. Mol. Biol.* 2012, *131*, 68–75.

[85] Im, G., Coculture in Musculoskeletal Tissue Regeneration. *TISSUE Eng. Part B* 2014, *00*, 1–10.

[86] Wang, I.-N. E., Shan, J., Choi, R., Oh, S., Kepler, C. K., et al., Role of osteoblast–fibroblast interactions in the formation of the ligament-to-bone interface. *J. Orthop. Res.* 2007, *25*, 1609–1620.

[87] Burattini, S., Ferri, P., Battistelli, M., Curci, R., Luchetti, F., et al., C2C12 murine myoblasts as a model of skeletal muscle development: morpho-functional characterization. *Eur. J. Histochem.* 2004, *48*, 223–33.

[88] Ma, J., Goble, K., Smietana, M., Kostrominova, T., Larkin, L., et al., Morphological and functional characteristics of three-dimensional engineered bone-ligament-bone constructs following implantation. *J. Biomech. Eng.* 2009, *131*, 101017.

[89] Larkin, L. M., Calve, S., Kostrominova, T. Y., Arruda, E. M., Structure and Functional Evaluation of Tendon–Skeletal Muscle Constructs Engineered in Vitro. *Tissue Eng.* 2006, *12*, 3149–3158.

[90] Kostrominova, T. Y., Calve, S., Arruda, E. M., Larkin, L. M., Ultrastructure of myotendinous junctions in tendon-skeletal muscle constructs engineered in vitro. *Histol. Histopathol.* 2009, *24*, 541–550.

[91] Shah, K., Majeed, Z., Jonason, J., O'Keefe, R. J., The role of muscle in bone repair: The cells, signals, and tissue responses to injury. *Curr. Osteoporos. Rep.* 2013, *11*, 130–135.

[92] Riley, L. A., Esser, K. A., The Role of the Molecular Clock in Skeletal Muscle and What It Is Teaching Us About Muscle-Bone Crosstalk. *Curr. Osteoporos. Rep.* 2017, 222–230.

[93] Guo, B., Zhang, Z. K., Liang, C., Li, J., Liu, J., et al., Molecular Communication from Skeletal Muscle to Bone: A Review for Muscle-Derived Myokines Regulating Bone Metabolism. *Calcif. Tissue Int.* 2017, *100*, 184–192.

[94] Wood, C. L., Pajevic, P. D., Gooi, J. H., Osteocyte secreted factors inhibit skeletal muscle differentiation. *Bone Reports* 2017, *6*, 74–80.

[95] Garvin, J., Qi, J., Maloney, M., Banes, A. J., Novel system for engineering bioartificial tendons and application of mechanical load. *Tissue Eng.* 2003, *9*, 967–79.

[96] Sawadkar, P., Alexander, S., Tolk, M., Wong, J., McGrouther, D., et al., Development of a surgically optimized graft insertion suture technique to accommodate a tissue-engineered tendon in vivo. *Biores. Open Access* 2013, *2*, 327–35.

Table 1: Medium compositions

Growth Medium Designation	Components
M1 - Skeletal Muscle Precursor maintenance medium:	– Dulbecco's Modified Eagle Media (DMEM) - High-Glucose (Hyclone) – 20% Foetal Bovine Serum (FBS) (PAN Biotech) – 1% Penicillin/Streptomycin (PS) (10,000U/mL and 10,000µg/mL, Gibco) – Eagle's Minimum Essential Medium (EMEM) - Earle's Balanced Salt Solution (EBSS) (Sigma)
M2 - Human Osteosarcoma maintenance medium:	– 10% FBS – 1% L-Glutamine (200mM, Sigma) – 1% Non-Essential Amino Acids (NEAA) (100x, Sigma) – 1% PS
M3 - Osteoblast-like cell maintenance medium:	– DMEM - Low-Glucose (Sigma) – 10% FBS – 1% PS
MM - Myogenic Medium:	– DMEM (High Glucose) – 2% Horse Serum – 1% PS
OM - Osteogenic Medium:	– DMEM (Low Glucose) – 10% FBS – 0.1µM Dexamethasone (Sigma) – 0.05mM Ascorbic acid (Sigma) – 10mM β-glycerol-phosphate (Sigma) – 1% L-Glutamine – 1% PS

Table 2: Quantitative reverse transcription polymerised chain reaction (qRT-PCR) Primers

Target mRNA (M-mouse; H- human)	Primer sequences 5'-3'		Reference Sequence Accession Number
	Forward	Reverse	
POLR2B (M)	GGTCAGAAGGGAACTTGTGGTAT	GCATCATTAAATGGAGTAGCGTC	NM_153798.2
POLR2B (H)	AAGGCTTGGTTAGACAACAG	TATCGTGGCGGTTCTTCA	NM_000938.1
Myogenin (M)	CCAACTGAGATTGTCTGTC	GGTGTTAGCCTTATGTGAAT	NM_031189.2
RUNX2/CBFa1 (H/M)	GCAGTATTTACAACAGAGGG	TCCCAAAAGAAGTTTTGCTG	NM_001145920
Osteocalcin/BGLAP(H)	CTCACACTCCTCGCCCTATT	TCCCAGCCATTGATACAGGT	NM_199173

Figure Legends

Figure 1: Monolayer co-culture systems. Each cell type was separated by a PDMS boundary with secreted and degradation products shared within the medium. Both cell types exposed to a single medium by filling the well to a volume above the height of the boundary.

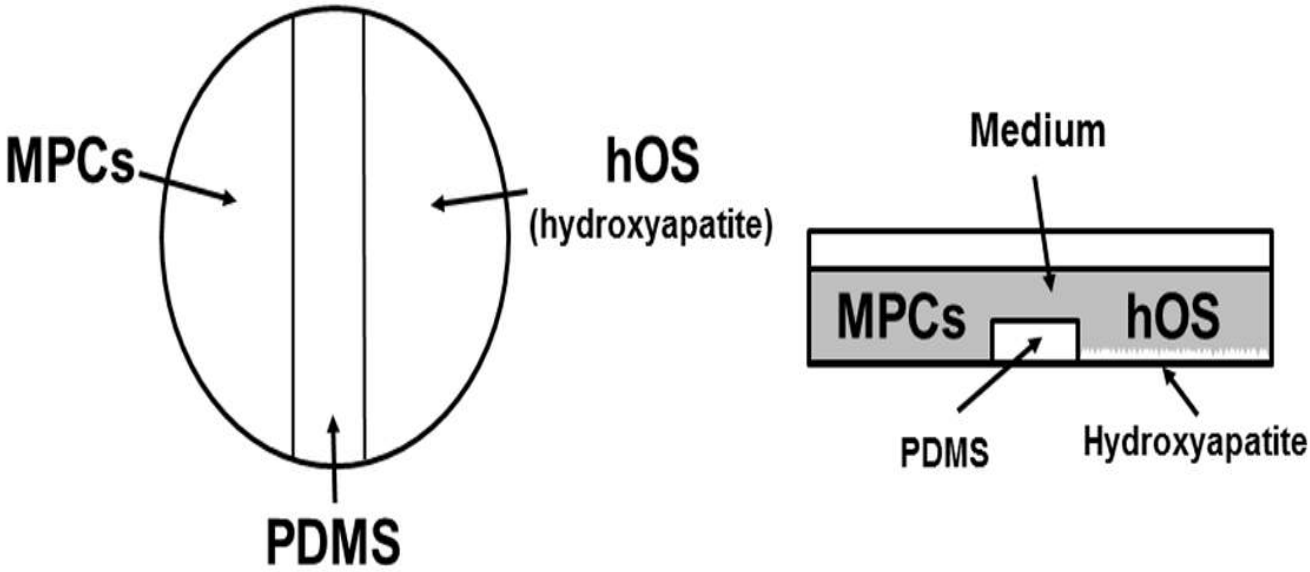

Figure 2: Schematic of 3D tissue engineered co-culture system. (Image left) To create the bone construct setting area, the threaded section of a 15 mL centrifuge tube was removed and placed on a PDMS-coated well. The ring was then sealed to the PDMS with 2.0mg/mL collagen. A minutien pin was placed in the centre of the ring to act as an anchor point for the bone construct. A PDMS boundary was placed adjacent to the ring and sealed with collagen. Not to scale. (Image right) 3D skeletal muscle and bone constructs after 14 days culture. Scale bar – 5mm

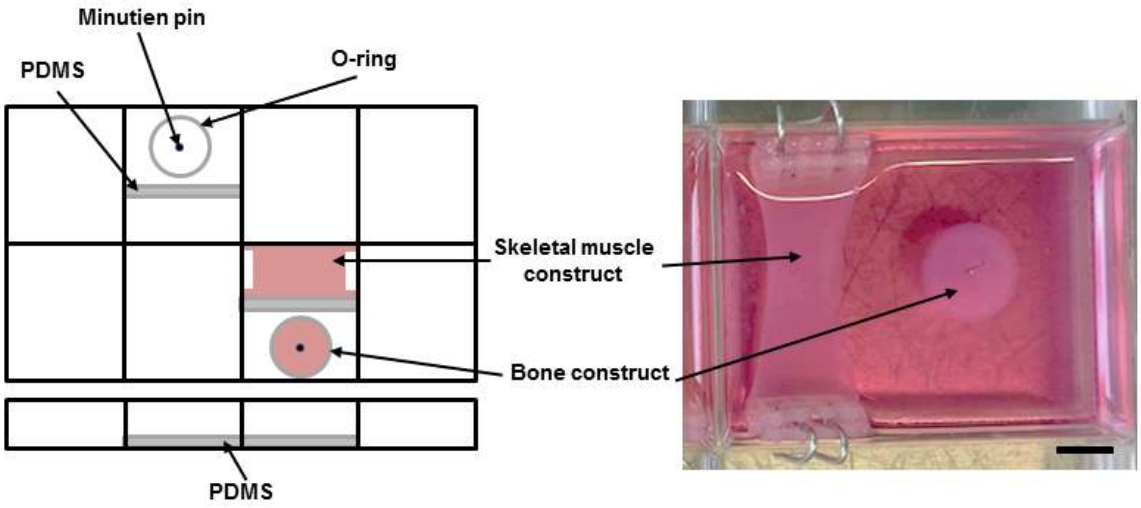

Figure 3: C2C12 and TE85 growth medium composition comparisons. DNA (A, B) and protein concentrations (C, D). (E, F) Protein/DNA ratios. 96h metabolic activity/live cell number (G, H). (I, J) 96h Viability (membrane integrity). n=3 per timepoint per condition + 3 replicates per well. * = $P<0.05$, ** = $P<0.01$, *** = $P<0.001$.

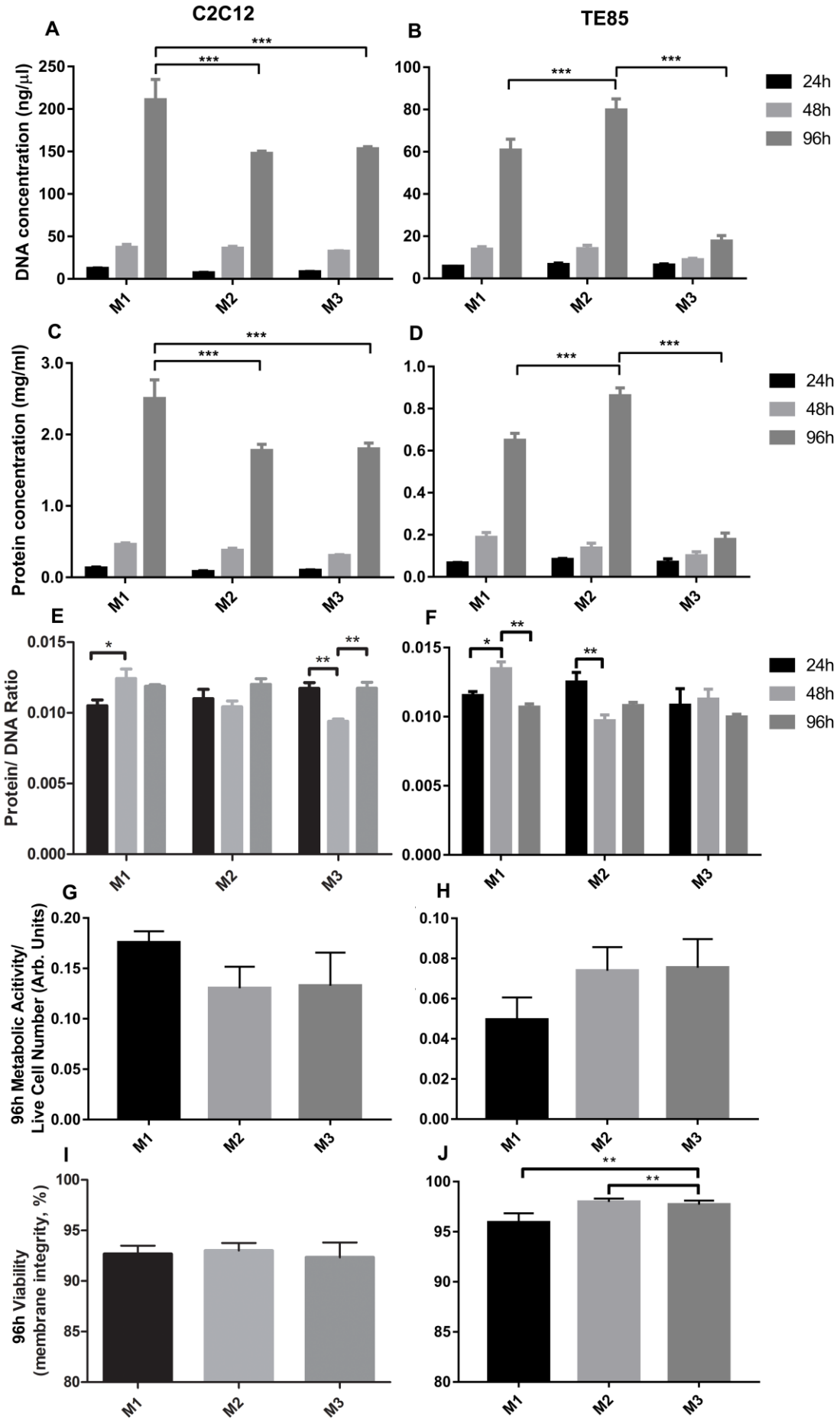

Figure 2: C2C12 (A-F, P-S) and TE85 (G-O, T-V) differentiation medium composition comparisons. (A-F) Monolayer C2C12 morphological observation. Desmin (red), DAPi (blue). Un-fused nuclei show little or no presence of desmin (denoted by →). (G-O) Brightfield images of TE85 human osteosarcoma cells after culture to confluency in M1 and then exposure to either myogenic or osteogenic medium (M2 +osteogenic medium control). (P) DNA concentrations in C2C12 cultures. (Q) Protein/DNA ratios. Real time qRT-PCR ($2^{-\Delta\Delta CT}$) profiles of myogenic and osteogenic markers. (R) Myogenin expression and (S) RUNX2/CBF-α1 expression of C2C12 cells in myogenic and osteogenic medium. TE85 culture's after 3 days (T) DNA concentrations (U) protein/DNA ratios. (V) RUNX2/CBF-α1 expression of TE85 cultures in myogenic and osteogenic. Scale bar – 50µm, n=3 culture replicates + 3 repeat measures for all conditions, * = p<0.05, ** = p<0.01, *** = p<0.001., **** = p<0.0001

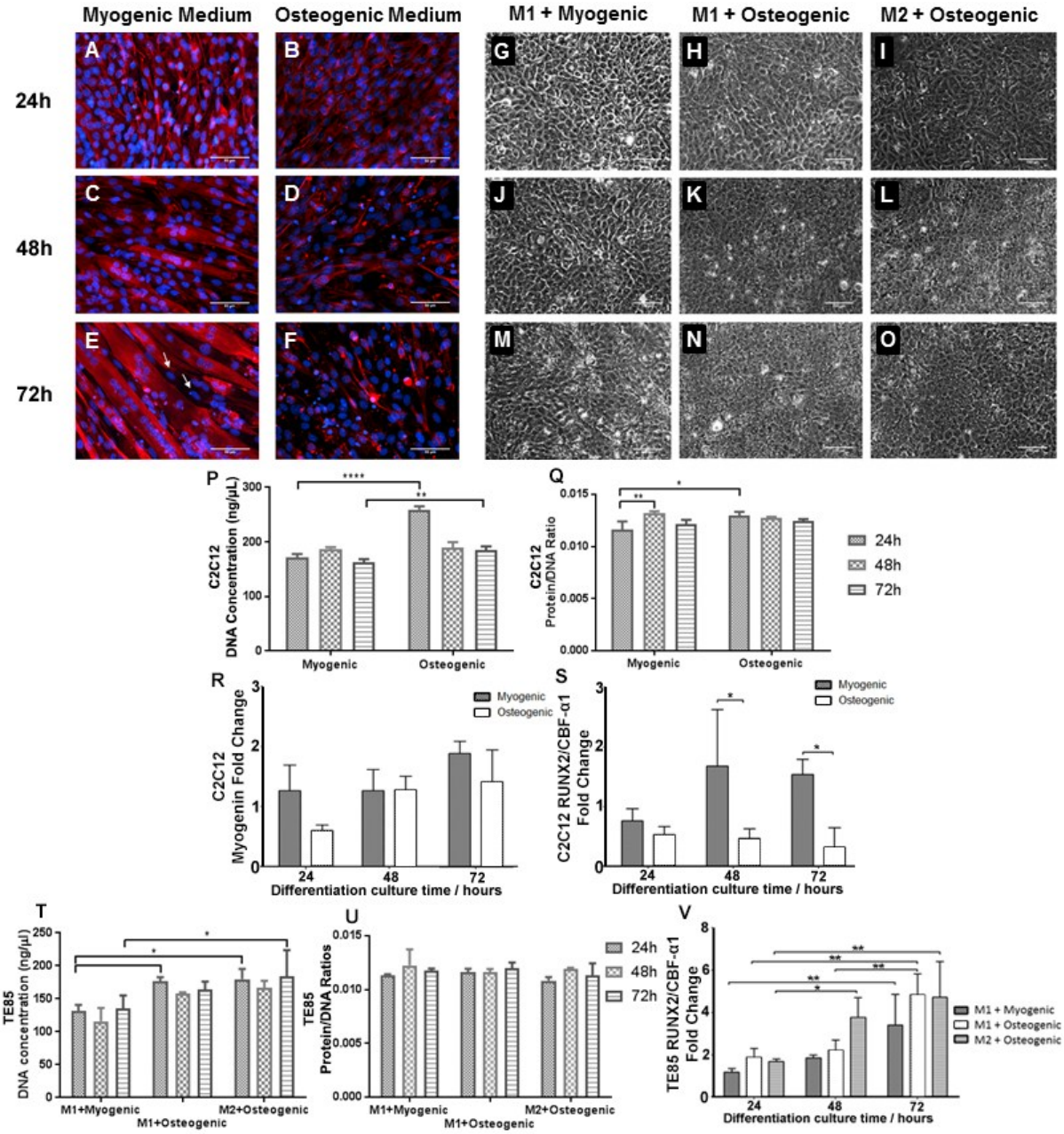

Figure 5: Monolayer co-culture differentiation: TE85 cell population DNA quantification and ALP/DNA ratio after 7 days culture (4 days in growth medium + 3 days in differentiation medium). (A) DNA Concentrations. (B) ALP/DNA ratios. Immunofluorescent images of (C) C2C12 (D) C2C12+HA conditioned media (E) C2C12/TE85 –HA (F) C2C12/TE85 +HA. Blue – Nuclei (DAPI), Red – F-actin (Rhodamine Phalloidin), Green – Desmin (Chromeo 488). Scale bar – 20µm. (G) Mean number of myotubes per image. (H) Fusion Index per image. (I) Mean nuclei per myotube per image. n=3 replicate cultures + 3 repeat measures, * = p<0.05, ** = p<0.01, *** = p<0.001, bars represent ±SD

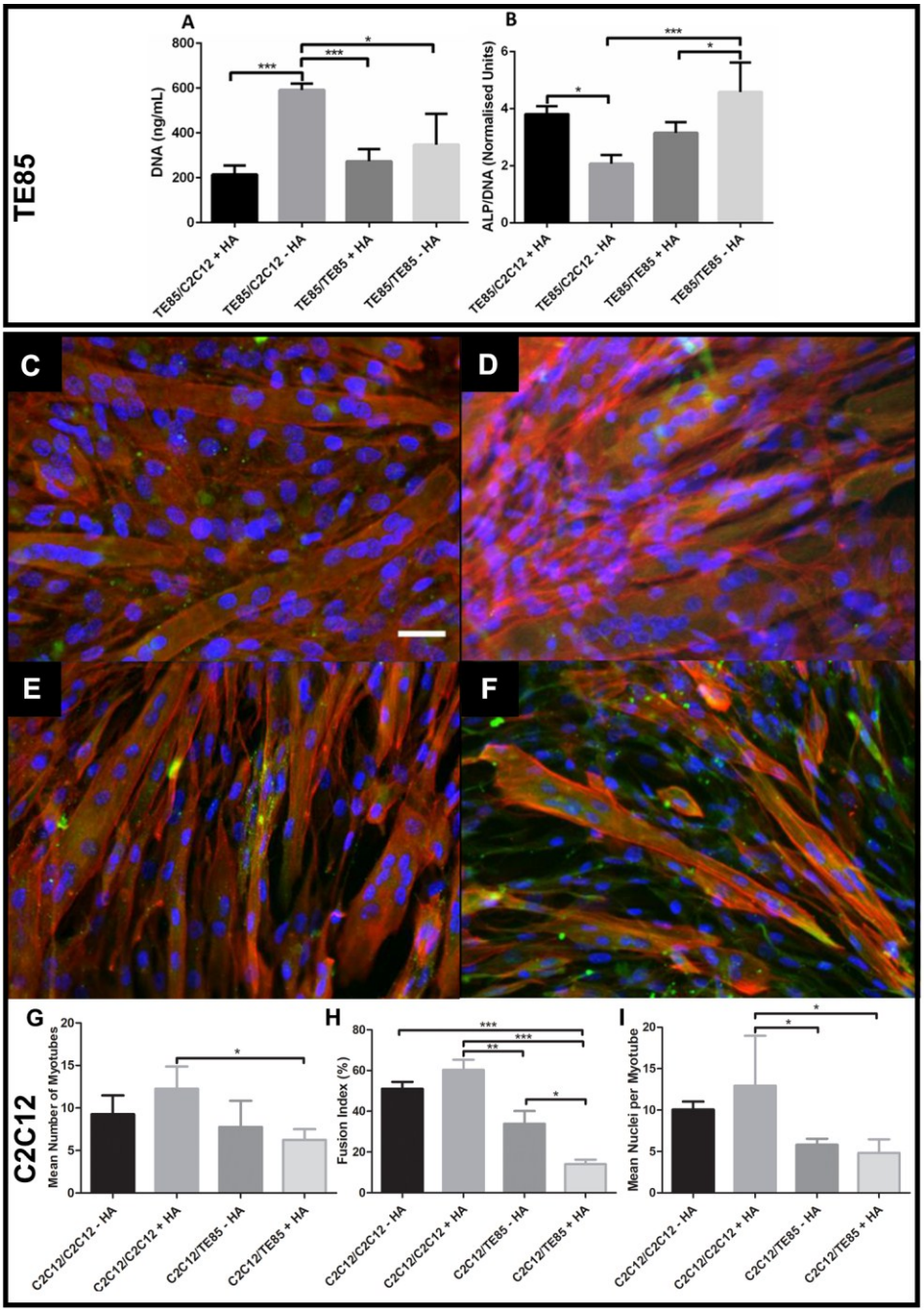

Figure 6: 3D skeletal muscle and bone co-culture: Real time qRT-PCR ($2^{-\Delta\Delta CT}$) measurement of RUNX2/CBF-α1 (A), Osteocalcin/BGLAP (B) and ALP/DNA ratios (C) in co-culture and bone model only controls. Immunofluorescence of (D) skeletal muscle only constructs myotubes, (E) aligned myotubes within a skeletal muscle construct co-cultured with bone constructs (fluorescence interference from collagen matrix) and (F) fused and unfused C2C12s within a skeletal muscle construct co-cultured with bone constructs. Blue – Nuclei, Red – Desmin. Scale bar- 100µm. Image analysis of myotube characteristics (G) Max myotube length. (H) Mean myotube length. (I) Number of myotubes per image. n=4 repeat conditions + 3 repeat measures, * p ≤ 0. 05, *** = p<0.001, bars represent ±SD.

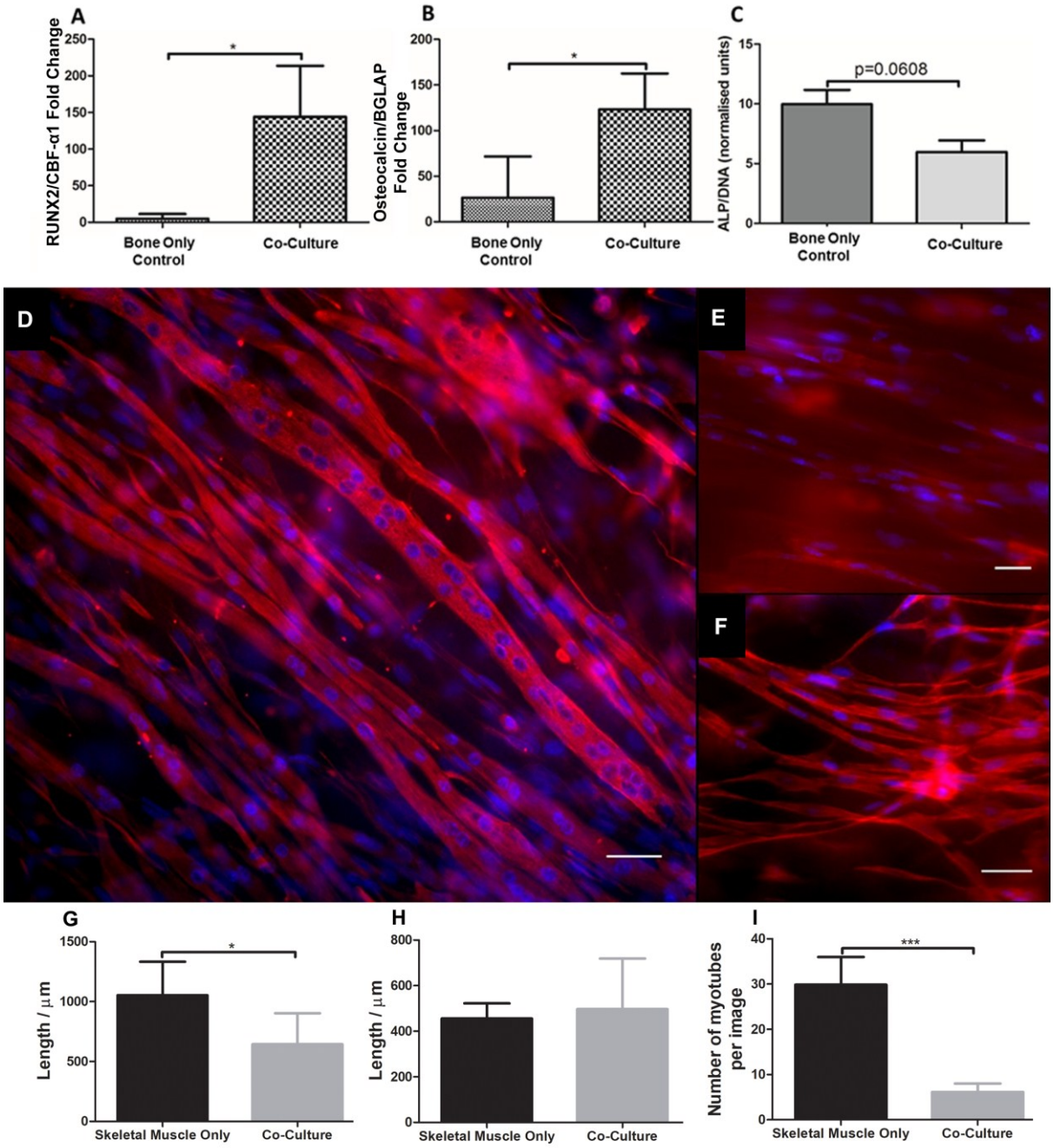

Laboratory-based 3D structures of individual tissues have been shown to better represent native tissue morphology and biochemical pathways than cells grown in a single layer. As a step towards creating a musculoskeletal junction, in this study, the authors demonstrate the culture conditions to enable to the formation of both skeletal muscle and bone constructs. Furthermore, the indicators of osteogenic differentiation were found to be increased in the present of skeletal muscle, whereas, in contrast, skeletal muscle myogenesis was found to be reduced. This work can form a basis for assessing toxicity of materials intended for use in the musculoskeletal system and as a platform to create a skeletal muscle-tendon-bone unit.